

Computer modelling of trivalent metal dopants in lithium niobate

This article has been downloaded from IOPscience. Please scroll down to see the full text article.

2008 J. Phys.: Condens. Matter 20 035201

(<http://iopscience.iop.org/0953-8984/20/3/035201>)

View [the table of contents for this issue](#), or go to the [journal homepage](#) for more

Download details:

IP Address: 129.252.86.83

The article was downloaded on 29/05/2010 at 07:25

Please note that [terms and conditions apply](#).

Computer modelling of trivalent metal dopants in lithium niobate

Romel M Araujo¹, Mário E G Valerio¹ and Robert A Jackson^{2,3}

¹ Physics Department, Federal University of Sergipe, Campus Universitário, 49100-000 São Cristóvão, SE, Brazil

² Lennard-Jones Laboratories, School of Physical and Geographical Sciences, Keele University, Keele, Staffordshire ST5 5BG, UK

E-mail: raraujo@fisica.ufs.br, mvalerio@fisica.ufs.br and r.a.jackson@chem.keele.ac.uk

Received 24 August 2007, in final form 12 November 2007

Published 10 December 2007

Online at stacks.iop.org/JPhysCM/20/035201

Abstract

Lithium niobate is a material with many important technological applications, and some of these applications are enhanced by doping the material with trivalent transition metal ions. This paper presents a computational analysis of the doping of lithium niobate by Sc, Cr, Fe and In. It is found that the preferred doping mechanism for Sc, Cr and Fe is a self-compensation mechanism (simultaneous substitution of the dopant at the Li and Nb sites), except for In, which shows a slight preference for substitution at the Nb⁵⁺ site with Nb–Li antisite compensation at 0 K. Cr and Fe doping have been studied experimentally, and the experimental findings support the predictions of the calculations regarding optimal doping sites in the material.

1. Introduction

Lithium niobate, LiNbO₃, is a material of great technological importance, with many applications in devices that exploit its properties, ranging from elastic to photorefractive [1–4]. Computer modelling provides a useful means of determining the properties of the material, including its defect chemistry, and the effect of doping on the structure. Previous papers have presented a new potential model for the material [5], and reported the doping of the structure by rare earth ions [6, 7].

In this paper, doping by Sc, Cr, Fe and In has been considered. These elements were chosen because they are of particular technological interest as dopants in LiNbO₃. Sc doping has been found to increase the photo-damage threshold [8]. It was also found that for Sc doping levels of 0.4 mole% or higher, no photorefractive damage was observed [9]. In addition, co-doping by In and Sc also increases the photo-damage threshold [10]. For LiNbO₃:Cr:Cu crystals, a non-volatile holographic recording can be obtained, and an appropriate Cr doping level helps improve the holographic recording properties [11]. In a very recent paper, Cr has been suggested as a versatile probe for mapping ferroelectric domain inversion in LiNbO₃ [12]. The authors of this paper also noted that Cr is found in two different site symmetries in LiNbO₃, which will be discussed later in the light of results presented. The effect of neutron irradiation on photorefractive

gratings in LiNbO₃:Fe single crystals has been studied, and it was found that excited electrons erase previously recorded holographic gratings [13]. In a recently published paper [14], x-ray absorption near edge structure spectroscopy has been used to study both the charge and location of Fe ions in LiNbO₃. The paper finds that Fe has the 3+ charge state, and that the Fe³⁺ ions are located at the Li⁺ sites. They also found that for Fe doping levels of 4.0 wt% or higher, a trivalent iron oxide co-phase was formed.

In the present paper, a computational study of doping LiNbO₃ by Sc, Cr, Fe and In is reported. Solution energies are calculated for doping with these ions, which enable predictions to be made of the preferred dopant sites and charge compensation mechanisms in the material.

2. Methodology

The application of computer modelling techniques to study the defect chemistry of solid state materials is widely established; recent applications to technologically important materials have included topaz, used in dosimeter devices [15], and LiCaAlF₆/LiSrAlF₆ [16] and BaY₂F₈ [17] used as solid state laser materials. Use is made of the Mott–Littleton method [18] in which point defects are considered to be at the centre of a region in which all interactions are treated explicitly, while approximate methods are employed for regions of the lattice more distant from the defect. The calculations were performed

³ Author to whom any correspondence should be addressed.

Table 1. Interionic potentials obtained from a fit to trivalent oxide structures.

Interaction	A_{ij} (eV)	ρ_{ij} (Å)	C_{ij} (eV Å ⁶)
Cr–O	1267.38	0.3197	3.65
Sc–O	1574.95	0.3231	4.67
Fe–O	1438.60	0.3148	3.58
In–O	1459.05	0.3347	5.24

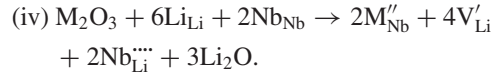
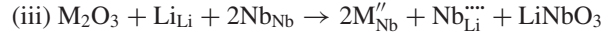
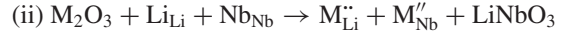
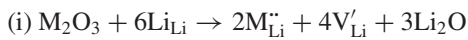
Table 2. Basic defect formation energies and lattice energies.

(a) Basic defect formation energies (per defect) (eV)		
	0 K	293 K
V'_{Li}	9.81	9.71
V''''_{Nb}	127.56	127.45
V''_O	18.98	18.91
Li'_i	-7.08	-7.12
Nb''''_i	-104.12	-104.25
O''_i	-9.47	-9.64
Nb''''_{Li}	-98.37	-98.49
(b) Lattice energies (eV)		
LiNbO ₃	-174.57	-174.66
Li ₂ O	-33.16	-32.92
Nb ₂ O ₅	-314.37	-313.99
Sc ₂ O ₃	-144.70	-144.77
Cr ₂ O ₃	-152.44	-152.52
Fe ₂ O ₃	-151.55	-151.63
In ₂ O ₃	-140.65	-140.76

using the GULP code [19]. The potentials for the dopant ion–oxygen interactions were obtained by fitting to the parent oxide structures, and are given in table 1.

3. Results and discussion

The trivalent dopant ions can potentially be incorporated at either the Li⁺ or the Nb⁵⁺ site, and the following possible defect reactions are considered in this paper (Kröger–Vink notation has been employed):



The first reaction involves substitution at the Li⁺ site, with charge compensation respectively by Li⁺ vacancies; the second involves self-compensation (substitution at both sites), and the third and fourth reactions involve substitution at the Nb⁵⁺ site with compensation by, respectively, Nb–Li antisite defects, and a combination of these and Li⁺ vacancies.

The energies corresponding to these reactions (E_{sol} , solution energies) are determined as follows:

$$(i) E_{sol} = -E_{latt}(M_2O_3) + E(2M'_{Li} + 4V'_{Li}) + 3E'_{latt}(Li_2O)$$

$$(ii) E_{sol} = -E_{latt}(M_2O_3) + E(M'_{Li} + M''_{Nb}) + E_{latt}(LiNbO_3)$$

$$(iii) E_{sol} = -E_{latt}(M_2O_3) + E(2M''_{Nb} + Nb''''_{Li}) + E_{latt}(LiNbO_3)$$

$$(iv) E_{sol} = -E_{latt}(M_2O_3) + E(2M''_{Nb} + 4V'_{Li} + 2Nb''''_{Li}) + E_{latt}(Li_2O).$$

Basic defect formation energies and lattice energies required to calculate the solution energies are given in table 2. In each of the above equations, the second term represents the formation energy of the dopant ion plus any charge compensating defect. These formation energies are tabulated, for each of the four dopants, in table 3. Bound defect formation energies have been calculated by including any defect binding present when the defect is formed. Solution energies are given in table 4. As with the defect formation energies, the bound solution energies include defect binding energies.

It can be seen from the bound solution energies presented in table 4(b) that the preferred solution mechanism for three of the four dopants involves solution at both Li⁺ and Nb⁵⁺ sites for both temperatures, while In³⁺ shows a slight preference for substitution at the Nb⁵⁺ site with Nb–Li antisite compensation at 0 K. This information is important in technological applications of the doped material, in that the material properties will be directly affected by both the dopant site and the form of charge compensation, if any. It would also be interesting to see if the predicted results for In³⁺ doping could be confirmed in a future experimental study.

Table 3. Defect formation energies.

Defect	2M(Li) + 4V(Li)		M(Li) + M(Nb)		2M(Nb) + Nb(Li)		2M(Nb) + 4V(Li) + 2Nb(Li)	
	0	293	0	293	0	293	0	293
(a) Unbound defects								
Sc	-34.26	-34.88	33.38	33.16	41.89	41.55	-17.24	-18.10
Cr	-42.70	-43.22	25.61	25.44	34.79	34.45	-24.34	-25.20
Fe	-41.80	-42.36	26.39	26.21	35.45	35.13	-23.68	-24.52
In	-29.74	-30.38	37.66	37.41	45.93	45.55	-13.20	-14.10
(b) Bound defects								
Sc	-36.02	-38.23	30.65	31.88	31.38	34.38	-30.61	-30.36
Cr	-44.81	-47.11	22.58	24.14	24.08	26.51	-36.62	-34.44
Fe	-43.85	-46.18	23.34	24.91	24.83	26.32	-40.28	-36.32
In	-31.47	-33.45	35.35	36.10	35.34	37.45	-26.18	-26.45

Table 4. Solution energies (per dopant ion).

Defect	2M(Li) + 4V(Li)		M(Li) + M(Nb)		2M(Nb) + Nb(Li)		2M(Nb) + 4V(Li) + 2Nb(Li)	
	0	293	0	293	0	293	0	293
(a) Unbound defects								
Sc	5.48	5.57	1.76	1.64	6.01	5.83	13.99	13.96
Cr	5.13	5.27	1.74	1.65	6.33	6.16	14.31	14.28
Fe	5.14	5.26	1.69	1.59	6.22	6.06	14.20	14.18
In	5.72	5.81	1.87	1.76	6.01	5.83	13.99	13.95
(b) Bound defects								
Sc	4.60	3.89	0.39	1.00	0.75	2.25	7.31	7.83
Cr	4.08	3.33	0.22	1.00	0.97	2.19	8.17	9.66
Fe	4.11	3.34	0.16	0.94	0.91	1.65	5.90	8.28
In	4.85	4.27	0.72	1.10	0.71	1.77	7.50	7.77

In the case of Cr doping, the results in table 4(b) are consistent with the findings of [12], where the Cr is seen to occupy two sites with different site symmetries (the lowest solution energy corresponds to simultaneous occupation of the Li and Nb sites). Similarly, Fe is also predicted to substitute at both Li and Nb sites, and this observation can explain the results of [14], where a co-precipitation of an iron oxide phase was observed for higher Fe dopant concentrations. This can only happen if both Li and Nb sites are occupied in the same region of the crystal.

4. Conclusions

The paper has presented a survey of doping of LiNbO₃ by transition metal ions, and predictions have been made of the energetically optimum sites for location of these dopant ions. In addition, the predictions of the present study are in line with those of recent experimental work in this field.

Acknowledgments

The authors are grateful to CNPq, FINEP, CAPES and the Royal Society for financial support.

References

- [1] Jazbinšek M and Zgonik M 2002 *Appl. Phys. B* **74** 407
- [2] Räuber A 1978 *Current Topics in Materials Science* vol 1, ed E Kaldis (Amsterdam: North-Holland) p 481
- [3] Prokhorov A M and Kuz'minov Yu S 1990 *Physics and Chemistry of Crystalline Lithium Niobate* 1st edn (New York: Hilger)
- [4] Wong K K (ed) 2004 *Properties of Lithium Niobate* (Piscataway, NJ: IEE)
- [5] Jackson R A and Valerio M E G 2005 *J. Phys.: Condens. Matter* **17** 837
- [6] Araujo R M, Lengyel K, Jackson R A, Valerio M E G and Kovacs L 2007 *Phys. Status Solidi c* **4** 1201–4
- [7] Araujo R M, Lengyel K, Jackson R A, Kovacs L and Valerio M E G 2007 *J. Phys.: Condens. Matter* **19** 046211
- [8] Zhen X, Li Q, Wang L and Xu Y 2005 *J. Cryst. Growth* **284** 270–4
- [9] Nakamura M, Takekawa S, Liu Y and Kitamura K 2005 *J. Cryst. Growth* **281** 549–55
- [10] Xu Z P, Xu S W, Xu Y H and Wang R 2005 *Mod. Phys. Lett. B* **19** 1277–84
- [11] Guo Y J, Liu L R, Liu D, Deng S G and Zhi Y N 2005 *Appl. Opt.* **44** 7106–11
- [12] Dierolf V and Sandmann C 2007 *J. Lumin.* **125** 67–79
- [13] Mandula G, Rupp R A, Balasko M and Kovacs L 2005 *Appl. Phys. Lett.* **86** 141107
- [14] Olimov Kh, Falk M, Buse K, Woike Th, Hormes J and Modrow H 2006 *J. Phys.: Condens. Matter* **18** 5135
- [15] Jackson R A and Valerio M E G 2004 *J. Phys.: Condens. Matter* **16** S2771
- [16] Amaral J B, Plant D F, Valerio M E G and Jackson R A 2003 *J. Phys.: Condens. Matter* **15** 2523
- [17] Amaral J B, Couto dos Santos M A, Valerio M E G and Jackson R A 2005 *Appl. Phys. B* **81** 841
- [18] Mott N F and Littleton M J 1938 *Trans. Faraday Soc.* **34** 485
- [19] Gale J D 1997 *J. Chem. Soc. Faraday Trans.* **93** 629